Origin of the incommensurate modulation of the 80-K superconductor $Bi_2Sr_2CaCu_2O_{8.21}$ derived from isostructural commensurate $Bi_{10}Sr_{15}Fe_{10}O_{46}$

Y. Le Page and W. R. McKinnon
Division of Chemistry, National Research Council of Canada, Ottawa, Canada K1A 0R9

J.-M. Tarascon and P. Barboux
Bell Communications Research, 331 Newman Springs Road, Red Bank, New Jersey 07701
(Received 5 December 1988; revised manuscript received 26 May 1989)

The compound $Bi_{10}Sr_{15}Fe_{10}O_{46}$ is shown to be isostructural with the 80-K superconductor $Bi_2Sr_2CaCu_2O_{8.21}$. The incommensurate modulation of the Cu compound is commensurate in the crystal of the Fe compound that was selected. The modulation is caused by the insertion of extra oxygen atoms in the Bi layers and results in corrugated slabs. The structure of the Bi-O layers can be described as roughly 70% of rocksalt type and 30% of oxygen-deficient perovskite type. The results explain the excess oxygen in the superconductor, the mechanism causing the corrugation, and the inelastic bending property displayed by single crystals. They also reconcile apparently discrepant results about the oxygen distribution in the bismuth layers.

I. INTRODUCTION

The structures of the high-temperature superconductors $Bi_2Sr_2Ca_{n-1}Cu_nO_{2n+4}$ have an incommensurate modulation,[1-5] usually attributed to the ordering of short Bi–O bonds.[6] A recent contribution[7] describes the large displacements of the metal atoms in this modulation, but gives no clues about the stereochemical mechanism that causes it. As part of a systematic investigation of compounds isostructural with these superconductors, we prepared the compound $Bi_2Sr_3Fe_2O_{9+\delta}$ and solved its crystal structure.[8] The solution shows that the modulation is caused by the insertion of one oxygen in the Bi layer every five subcells. This extra oxygen also explains why there is a mixture of Fe^{3+} and Fe^{4+} (or Cu^{2+} and Cu^{3+} in the superconductor), and thus is the connection between the modulation and superconductivity in the Bi-Sr-Ca-Cu-O system.

II. SAMPLE PREPARATION

The phase was prepared in an alumina crucible, 1.2 cm in diameter and 5 cm high, containing 10 g of powder, composed of 56% Bi_2O_3, 35% $SrCO_3$, and 9% Fe by weight. The crucible was heated in a tubular furnace to 1200 °C in 5 h, held for 2 h, cooled to 800 °C in 60 h, then removed from the furnace. The surface of the charge indicated partial melting, and within the load were cavities containing transparent, dark brown platelets, ranging in size from several micrometers to a millimeter. Electron micrsocopy could not detect any stacking faults in these crystals. Measurements of the weight change of crystals heated in hydrogen in a thermogravimetric analysis (TGA) apparatus indicate an oxygen content of 45.75 ± 0.2.

Most platelets had mutually perpendicular striations on the large face, while a few had only parallel striations. Striations can be characteristic of crystal faces. We interpreted the mutually perpendicular striations as a likely indication of twinning by 90° rotation about [001], a twin operation by pseudomerohedry. A $0.26\times0.10\times0.01$ mm^3 sample showing parallel striations only was selected and turned out to be an orthorhombic crystal with space group $B222$ and cell parameters $a=27.245(9)$ Å, $b=5.4617(6)$ Å, and $c=31.696(4)$ Å. The plane of the platelet was (002) and the striations were along [010], a fact that should be helpful for the selection and orientation of single crystals for physical measurements.

III. SOLUTION OF THE STRUCTURE

These materials are insulators, not conductors, yet the similarity of their structure with that of $Bi_2Sr_2CaCu_2O_{8+\delta}$ is obvious from cell parameters and diffraction patterns. The nonconventional cell axes given earlier were chosen to preserve the conventional orientation of the orthorhombic subcell, and to allow direct comparison with previous literature results. But in the superconductor the modulation is incommensurate, with a period 4.76 times the substructure period along a, whereas here it is commensurate, five times the subcell period. This commensurability was established in two ways: First, the substructure and superstructure reflections are commensurate within the experimental error; second, all diffraction profiles are sharp, whereas in incommensurate modulations the superstructure reflections are usually broader than the substructure ones. Thus, both the substructure and the superstructure could be solved using standard crystallographic methods.

The essential details of x-ray diffraction intensity measurements and data reduction are given in Table I. Direct methods followed by least-squares refinement and difference-Fourier maps gave the atomic positions in Table II. Although the individual isotropic thermal pa-

TABLE I. Crystal data, data collection, and refinement.

Formula:	$Bi_{10}Sr_{15}Fe_{10}O_{46}$, $Z=4$
Space Group:	$B222$ #21 with axes relabeled
Cell parameters:	$a=27.245(9)$, $b=5.4617(6)$, $c=31.696$ (4)
Radiation:	Graphite-monochromated MO $K\alpha$
Diffractometer:	CAD-4 with profile display, 2 θ scan and on-line profile analysis
Reflections measured:	10437
Unique reflections:	3876
Observed:	1418
Absorption correction:	Gauss integration
R_{sym}:	7.0%
Independent atoms:	44
Number of parameters:	233
Refinement:	Full matrix on 3876 rflns, unit weights
RF on observed refs:	10.6%

rameters of oxygen atoms were refined, these parameters could be divided into two groups within the standard deviations or sigmas of the refinements: the "perovskite oxygens" O(B0) and O(B1) on one hand with a B (the mean-square vibration amplitude) of about 0.03 Å^2, and all the other oxygens on the other hand with a B value of about 0.01 Å^2. As we felt that the differences in the thermal motion from these average values were not significant, we fixed them to these values to decrease the total number of refinement parameters from 259 to 233.

All the reflections were sharp, but not split or otherwise irregular. Nevertheless, crystals like these with weak interlayer bonding are undoubtedly twinned by merohedry, which superposes Friedel pairs; to handle this, we merged the data according to mmm point-group symmetry and performed η refinement,[9] imposing equal amounts of the enantiomorphs.

The results of the refinements confirm the similarity of the iron compound with the copper compound. In the copper compound, the central plane of the perovskite block contains calcium but not oxygen; here it contains both strontium and oxygen, so the subcell contains nine oxygens, rather than eight. Consequently, the c parameter of the iron compound is longer, and all the iron atoms have a distorted octahedral environment.

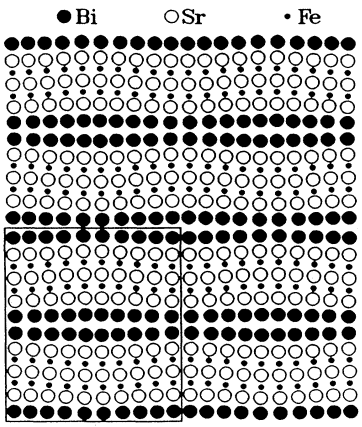

FIG. 1. Projection down the b axis of the positions of metal atoms. The origin is at the bottom left, with the x axis horizontal, and the z axis vertical. Two periods are plotted along each direction. The transverse sinusoidal oscillations of the slabs are perceptible, and the longitudinal compression and extension of the Bi layers can be perceived in the varying gap between the black Bi circles. Examination at grazing incidence along x and z enhances the perception of the deformations.

IV. THE MODULATION OF THE STRUCTURE

The atomic displacements of the metal atoms associated with the superstructure are so large that they can be

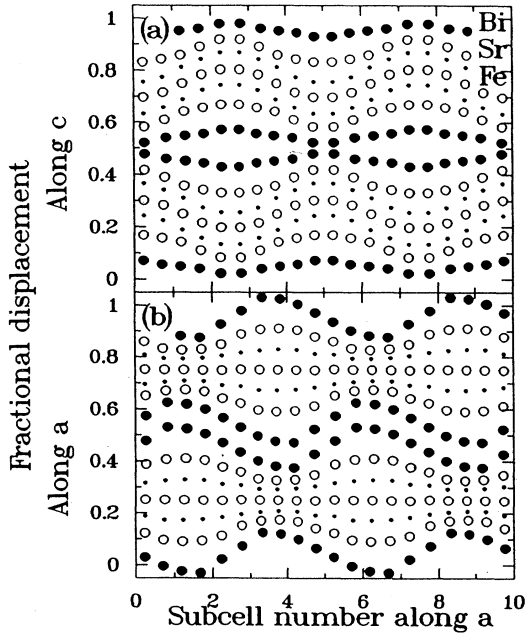

FIG. 2. This plot is to be compared directly with Figs. 2(a) and 2(b) in Gao *et al.*[7] The solid curves in Ref. 7 are dots here because our modulation is commensurate. The average vertical position of each row of atoms is the average z coordinate for that row. The displacements about this average are, for (a), five times the deviation of z from its average value, and, for (b), five times the deviation of x from its ideal values of 0.05, 0.15, 0.25, ... Since a and c are both about 30 Å, a deviation of 0.1 vertical unit in the figure corresponds to an atomic displacement of about 0.6 Å.

even in projections of the atom positions (Fig. 1). Qualitatively, the slabs of Sr-Fe-Sr-Fe-Sr flex sinusoidally along x as a solid unit, moving up and down in the z direction with amplitude 0.3 Å [Fig. 2(a)]. The Bi layers also flex, but less so. Just as in the elastic bending of a plate,[10] this flexing produces a periodic expansion and compression along a [Fig. 2(b)]. The amplitude of the expansion and compression is zero at the center of the slab (called the neutral surface in elasticity theory[10]), and increases with distance from the center.

This modulation is qualitatively the same as that described by Gao *et al.*[7] for the superconductor. In their Fig. 2(a), the two facing Bi layers around $z=\frac{1}{2}$ are corrugated with opposite phases, giving an apparently inefficient stacking. We observe here the same phenomenon. The main difference between their model and ours is that the modulations we observe is sinusoidal with little second harmonic contribution, and is slightly larger in amplitude. This difference is minor, however, and the two compounds can be considered to be isostructural.

The electron diffraction photographs of Matsui *et al.*[11] also show the same qualitative distribution of metal atoms as in Fig. 1, but considerably more distorted. In fact, the distortion visible in their Fig. 3 is so large that it probably corresponds to an imaging artifact or to a relax-

TABLE II. Atomic parameters x,y,z and B_{iso}. Estimated standard deviations refer to the last digit printed. The thermal motion of oxygen atoms was not refined.

Atom	mult	x	y	z	B_{iso}
Bi(1)	8	0.05511(19)	0.7678(8)	0.54251(9)	2.7(2)
Bi(2)	8	0.16544(12)	0.2360(11)	0.54618(10)	2.2(2)
Bi(3)	8	0.26429(9)	0.7671(7)	0.54786(10)	1.1(1)
Bi(4)	8	0.36031(10)	0.2251(6)	0.54938(7)	0.8(1)
Bi(5)	8	0.45354(10)	0.7660(6)	0.55235(8)	1.0(1)
Sr(1)	8	0.0540(3)	0.2488(17)	0.6221(4)	3.2(4)
Sr(2)	8	0.15765(20)	0.7465(12)	0.62757(20)	1.1(2)
Sr(3)	8	0.25837(19)	0.2451(17)	0.63403(23)	1.8(3)
Sr(4)	8	0.35717(17)	0.7414(12)	0.63708(18)	0.9(2)
Sr(5)	8	0.45176(22)	0.2500(14)	0.63938(19)	1.4(3)
Fe(1)	8	0.0513(4)	0.7509(21)	0.6783(3)	0.9(3)
Fe(2)	8	0.1528(3)	0.240(3)	0.6832(5)	2.0(5)
Fe(3)	8	0.2537(4)	0.730(3)	0.6894(4)	1.8(5)
Fe(4)	8	0.3533(3)	0.2452(16)	0.6968(4)	0.7(3)
Fe(5)	8	0.4504(4)	0.754(3)	0.7005(3)	1.3(4)
Sr($C1$)	8	0.44970(24)	0.2479(14)	0.76046(19)	1.0(3)
Sr($C2$)	8	0.34984(25)	0.7473(19)	0.7569(3)	1.9(3)
Sr($C3$)	4	$\frac{1}{4}$	0.256(3)	$\frac{3}{4}$	0.9(4)
O($B0$)	4	0	0	0.545(4)	3
O($B1$)	8	0.088(3)	0.070(16)	0.551(3)	3
O($B2$)	8	0.1865(18)	0.855(10)	0.5435(16)	1
O($B3$)	8	0.2738(16)	0.228(10)	0.5501(14)	1
O($B4$)	8	0.3675(18)	0.897(10)	0.5508(16)	1
O($B5$)	8	0.4597(17)	0.191(10)	0.5547(15)	1
O($S1$)	8	0.0582(16)	0.725(10)	0.6152(14)	1
O($S2$)	8	0.1702(16)	0.266(12)	0.6111(14)	1
O($S3$)	8	0.2589(16)	0.760(11)	0.6118(14)	1
O($S4$)	8	0.3586(17)	0.272(11)	0.6205(14)	1
O($S5$)	8	0.4515(18)	0.726(10)	0.6163(13)	1
O($FA1$)	4	0	0	0.6658(22)	1
O($FA2$)	8	0.1044(19)	0.022(11)	0.6800(16)	1
O($FA3$)	8	0.2023(18)	0.007(11)	0.6696(16)	1
O($FA4$)	8	0.3024(19)	0.994(11)	0.6900(16)	1
O($FA5$)	8	0.4043(19)	0.016(11)	0.6877(16)	1
O($FA6$)	4	$\frac{1}{2}$	0	0.6966(22)	1
O($FB1$)	4	0	$\frac{1}{2}$	0.6760(22)	1
O($FB2$)	8	0.1001(19)	0.489(11)	0.6725(16)	1
O($FB3$)	8	0.2057(18)	0.515(11)	0.6844(16)	1
O($FB4$)	8	0.3024(19)	0.497(12)	0.6825(16)	1
O($FB5$)	8	0.3992(19)	0.507(11)	0.6948(16)	1
O($FB6$)	4	$\frac{1}{2}$	$\frac{1}{2}$	0.6892(23)	1
O($C1$)	8	0.4524(19)	0.779(9)	0.7576(13)	1
O($C2$)	8	0.3494(18)	0.316(10)	0.7646(15)	1
O($C3$)	4	$\frac{1}{4}$	0.753(16)	$\frac{3}{4}$	1

ation of the structure due to the proximity of the surface. For example, in their Fig. 3, and its computer interpretation Fig. 6, some of the Bi-Sr-Cu-Ca-Cu-Sr-Bi rows are inclined by 13° from the c axis, about three times as much as the maximum inclination in the Fe compound in Fig. 1. Such large angles also contradict the results of Gao *et al.*,[7] which indicate that the distortion in $Bi_2Sr_2CaCu_2O_{8+y}$ is slightly less than in the present Fe analog. Also, some Bi-Sr-Fe-Sr-Fe-Sr-Bi rows are perceptibly curved in the electron-diffraction pictures, whereas the x-ray images show them to be very close to straight lines. In spite of these quantitative differences, however, the distortion of the metal atoms imaged in Ref. 11 is qualitatively the same as our x-ray results, for the slab architecture and for the stacking along c, when projected down b.

The distortion originates in the oxygen distribution. In the Sr-Fe-Sr-Fe-Sr slab, the oxygen occupies positions slightly distorted from a flexed perovskite structure. But in the bismuth layer, the oxygen is near one of two types of sites, which we call here rocksalt type and bridging type [Fig. 3(a)]. In the undistorted substructure, both these sites are unsatisfactory. At the bridging site, the oxygen is 1.9 Å away from two Bi atoms. Since an oxygen exchanges one valence unit[12] (v.u.) with a Bi at 2.09 Å, such an oxygen would have a valence exceeding 2. At the rocksalt site, an oxygen is 2.7 Å away from four Bi atoms, corresponding to only 0.8 v.u. One way to satisfy the oxygen valence is to move all the oxygens to positions between rocksalt and bridging sites, forming Bi–O chains or clusters.[7] But such a solution does not account for the flexing of the slabs nor for the extra oxygen content.

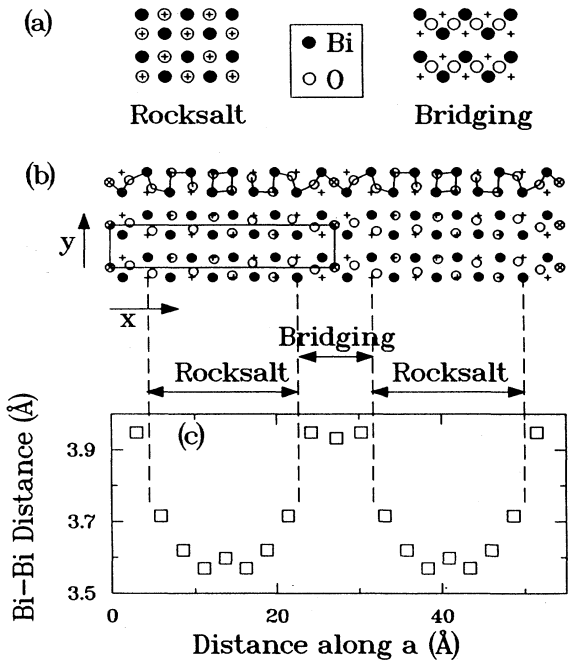

FIG. 3. (a) Ideal atom locations for the two competing types of planar arrangement of oxygen atoms, designated here rocksalt and bridging. The + signs indicate rocksalt positions throughout. (b) Section of the structure at $z=0.55$, through the Bi layer. Rocksalt and bridging-type regions are indicated. The modulation allows the insertion of an extra oxygen atom every ten Bi rows, indicated by an x. The bonds drawn in the upper part join each Bi to its two closest O neighbors in the Bi-O plane; each Bi also has a third short bond to an oxygen in the Sr-O layer undeneath (not shown). (c) Bi-Bi distances plotted with the same scale along x as in 3(b). With respect to the Bi-Bi distance of 3.86 Å in the subcell, the bridging type region is expanded and the rocksalt-type region is compressed.

The flexing is produced by the alternation of regions where oxygen lies near rocksalt positions with regions where it lies on or near bridging positions [Fig. 3(b)]. The rocksalt regions are compressed along the a direction to shorten the Bi-O distance, and the bridging regions are expanded to increase the Bi-O distance. This expansion and contraction is mirrored in the Bi-Bi distance [Fig. 3(c)], and is responsible for the flexing of the slabs.

The expansion and contraction also allows the Bi-O layer to accommodate extra oxygen atoms, explaining the oxygen stoichiometry of the compound. If we start from the undistorted substructure with flat slabs [Fig. 4(a)], with the oxygen in rocksalt positions [the crosses in Fig. 3(b)], we can produce the distortion by expanding one in every ten Bi-Bi distances and inserting an oxygen atom between those Bi atoms. The other oxygens in the Bi-O layer relax, with the two oxygens closest to the inserted oxygen moving almost to bridgings sites and expanding two other Bi-Bi dis;tances [Fig. 3(c)], and the other oxygens staying near the rocksalt positions. Pushing apart Bi atoms also pushes apart atoms in the perovskite slabs underneath, as if a wedge had been inserted into the slabs. The same feature occurs every ten Bi atoms. If no compensation occurred, the slab would curl up and make

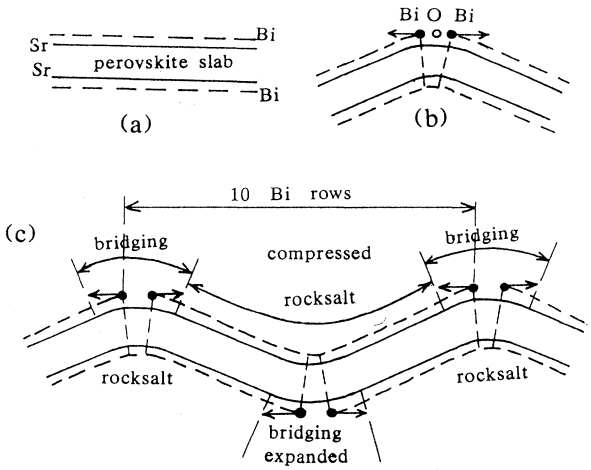

FIG. 4. Mechanism responsible for the transverse and longitudinal atomic displacements shown in Fig. 2. (a) Substructure with the perovskite slab lined on top and bottom by Bi layers. (b) Insertion of an oxygen atom in bridging positions in between two Bi atoms increases the Bi-Bi distance and bends the slab. (c) Insertion of oxygen atoms every ten rows on each face, in alternance for the two faces, causes transverse deformations of the perovskite slab, with associated longitudinal displacements that most affect the Bi layer.

cylindrical fibers similar to chrysotile. Fortunately, the second face of the slab is also lined with a similar Bi layer, but with the enlarged region midway between the enlarged regions of the first face. As a result, the slab bends up and down sinusoidally, but remains globally straight, and slabs can stack to form crystals.

This flexion also compresses the Bi-O layers midway between the expanded regions, pushing the oxygen and bismuth atoms together to distances which are appropriate for the establishment of bonds with the proper lengths in a rocksalt structure (Table III). Three of the Bi—O bond lengths refined shorter than 2Å and should not be accepted at face value. However, small displacements of these atoms by a few sigmas would bring these distances back to acceptable values. Each Bi atom has three short Bi—O bonds, two in the Bi-O layers and one to oxygen in the adjacent Sr-O layer, and the three short bonds are mutually perpendicular, in accordance with the known stereochemistry of Bi^{3+}.

V. COMPARISON WITH THE SUPERCONDUCTING Cu ANALOGUE

The preceding description corresponds to the iron compound. It also applies qualitatively to the isostructural cuprate superconductor $Bi_2Sr_2CaCu_2O_{8.21}$ although the stacking of the slabs in the superconductor is probably accompanied by a shift parallel to the b axis, based on the Amaa space group of the substructure.[7] The incommensurability of the modulation can be explained by a pseudoperiodicity of the inserted oxygen atoms, which can occur after ten Bi atoms or after nine Bi atoms, approximately at random according to the value of the q vector of $0.21a^*$. On electron-microscope photographs, where both sides of the slab are seen, this would produce gaps of five rows and gaps of four rows.

Thus the superstructure corresponds to the insertion of one oxygen for every ten Bi atoms, leading to the formula $Bi_{10}Sr_{14}Fe_{10}O_{46}$ in agreement with TGA measurements that indicate an oxygen content of 45.75 ± 0.2. The valence associated with this extra oxygen is probably accommodated in the iron layer, producing a mixture of Fe^{3+} and Fe^{4+}, or equivalently an average Fe valence between 3 and 4. Although there are many examples[13] of perovskites and related structures that contain Fe^{4+}, we cannot rule out from the structure alone that the extra valence is partly or fully taken up by Bi. Electronic structure calculations[14] using the atomic parameters of Table II, however, place the Bi-6s band well below the Fermi level and the Bi-6p band well above it, correspond-

TABLE III. Bi-O distances and angles at Bi for the three shortest distances.

Bi(1)-O(B0)	1.97(1)	O(B0)-Bi(1)-O(B1)	78(3)
Bi(1)-O(B1)	1.90(9)	O(B0)-Bi(1)-O(S1)	93(3)
Bi(1)-O(S1)	2.32(5)	O(B1)-Bi(1)-O(S1)	86(3)
Bi(1)-O(B0)	3.39(9)		
Bi(1)-O(B1)	3.23(8)		
Bi(1)-O(B2)	3.61(5)		
Bi(2)-O(B1)	2.30(8)	O(B1)-Bi(2)-O(B2)	82(3)
Bi(2)-O(B2)	2.16(5)	O(B1)-Bi(2)-O(S2)	91(3)
Bi(2)-O(S2)	2.07(5)	O(B2)-Bi(2)-O(S2)	96(2)
Bi(2)-O(B2)	3.43(5)		
Bi(2)-O(B2)	2.94(5)		
Bi(2)-O(B3)	2.95(4)		
Bi(3)-O(B2)	2.18(5)	O(B2)-Bi(3)-O(B3)	83(2)
Bi(3)-O(B3)	2.53(6)	O(B2)-Bi(3)-O(S3)	90(2)
Bi(3)-O(S3)	2.03(5)	O(B3)-Bi(3)-O(S3)	90(2)
Bi(3)-O(B3)	2.96(6)		
Bi(3)-O(B3)	3.12(5)		
Bi(3)-O(B4)	2.90(5)		
Bi(4)-O(B3)	2.36(5)	O(B3)-Bi(4)-O(B4)	97(2)
Bi(4)-O(B4)	1.80(5)	O(B3)-Bi(4)-O(S4)	88(2)
Bi(4)-O(S4)	2.27(4)	O(B4)-Bi(4)-O(S4)	95(2)
Bi(4)-O(B4)	3.25(5)		
Bi(4)-O(B4)	3.68(5)		
Bi(4)-O(B5)	2.72(5)		
Bi(5)-O(B5)	2.33(5)	O(B5)-Bi(5)-O(B5)	80(2)
Bi(5)-O(B5)	2.38(5)	O(B5)-Bi(5)-O(S5)	94(2)
Bi(5)-O(S5)	2.04(4)	O(B5)-Bi(5)-O(S5)	90(2)
Bi(5)-O(B4)	2.45(5)		
Bi(5)-O(B5)	3.15(5)		
Bi(5)-O(B5)	3.41(5)		

ing to Bi^{3+}. We do not know why the mixture of iron valences does not result in a conductor; perhaps the charges are ordered in some way, or islands of mixed-valence regions are separated by Fe^{3+} ions. Similarly, if the superconductor was commensurate, its formula would be $Bi_{10}Sr_{10}Ca_5Cu_{10}O_{41}$, but as it is incommensurate with a repeat distance of 4.76 substructure periods, one extra oxygen is inserted for every 9.52 Bi atoms, giving a formula of $Bi_2Sr_2CaCu_2O_{8.21}$, again in agreement with TGA measurements. This excess oxygen raises the copper valence to values between 2+ and 3+, empirically a prerequisite for superconductivity above 77 K.

The foregoing results reconcile apparently discrepant views about the oxygen distribution in the Bi plane of the superconductor.[2–6] As there are three long Bi-Bi distances and seven short ones in Fig. 3(b), we suggest that the Bi-O layer can be described roughly as 30% of an oxygen-deficient perovskite structure (where the oxygens occupy bridging sites), and 70% of the rocksalt structure. The short bonds within the Bi-O sheets link some of the Bi and O together into strings and the rest into isolated Bi_2O_2 clusters [Fig. 3(b)], so both possible configurations suggested in Ref. 6 for the Cu compound are realized in the Fe compound.

It is significant that no oxygen atom was found in Aurivillius-type positions between adjacent Bi-O layers. This absence explains why the crystals containing iron and copper bend inelastically, a characteristic that makes the diffraction study of their single crystals so difficult. Inelastic bending is an unusual property among oxides, and indicates that the structure contains slabs joined to one another only by weak bonds, usually van der Waals bonds, hydrogen bonds, or here, unusually weak ionic bonds. It also explains why characterizing these materials by powder diffraction is difficult; grinding causes the slabs to slip, and destroys the spatial coherence of the crystallites in the powder. The 00*l* reflections become prominent to the extent that cell parameters are difficult to obtain by the powder method.

Iron is mostly 3+ in $Bi_{10}Sr_{15}Fe_{10}O_{46}$, whereas Cu is mostly 2+ in $Bi_2Sr_2CaCu_2O_{8.21}$. The reason for this difference can be traced to the center of the perovskite slabs, where the Fe compound has a layer of SrO whereas the Cu compound has only a layer of Ca. This difference probably explains why the Fe compound has a lower density of stacking faults than the Cu compound has. Let us consider stacking faults where perovskite slabs from the $n=3$ phase (with three Cu or Fe layers are perovskite slabs) replace slabs from the $n=2$ phase. The energy of such stacking faults will be proportional to the difference in energy of the $n=2$ and $n=3$ phases. In the Cu compound, the $n=3$ phase is generated by introducing a CuO_2 layer and a Ca layer into the perovskite slabs of $n=2$ phase, for a net change of $CaCuO_2$. Since the Cu valence is near 2+ in the $n=2$ phase, this pair of layers is almost balanced in valence, so its introduction does not change the net Cu valence by much. In contrast, the $n=3$ phase of Fe is presumably generated from the $n=2$ phase by introducing a layer of FeO_2 and a layer of SrO, for a net change of $FeSrO_3$. This pair of layers has a net valence 1− per Fe atom if Fe has a valence 3+, so adding it will change the average Fe valence, at an associated cost in energy. Thus the energy difference between the $n=3$ and $n=2$ phase of Fe is expected to be significantly higher than for Cu, and the density of stacking faults correspondingly lower. Moreover, it should be easier in the case of Fe to prepare the $n=3$ phase without contamination from the $n=2$ phase than it is in the case of Cu, as we observe experimentally.[15]

As this discussion of stacking faults shows, differences between the Fe and Cu compounds can be traced to the differences in the center of the perovskite slabs. The distortion that causes the superstructure, on the other hand, originates in a different part of the structure, the Bi-O layers. Since the Bi-O layers are common to both the Fe and Cu compounds, we expect that the structural distortion will have a common origin. The similarity between the metal atom displacements for the Fe compound in Fig. 2 and those for the Cu compound in Ref. 7 emphasizes this point. Since the distortion is caused by the insertion of extra oxygen in the Bi-O layers, we see the connection between the distortion and superconductivity in the Cu compound: The extra oxygen in the Bi-O layers that causes the distortion also produces the electronic carriers (holes or Cu^{3+}) that form Cooper pairs in the CuO_2 layers.

After this work was submitted, we received a paper by Hewat *et al.*[16] proposing an explanation for the superstructure of $Bi_2Sr_2CaCu_2O_{8.2}$ in terms of a model of oxygen insertion in the Bi layers. The speculative model shown in their Fig. 4 is similar to our observations in Fig. 3, in that it shows an oxygen on a twofold axis parallel to *c*, at the top of the wave of corrugation. With oxygen on a twofold axis, there must by symmetry be an odd number of oxygens in bridging positions, as we find. On the other hand, one can imagine a second possibility, in which the Bi atoms lie on a mirror plane; in this case, there would be an even number of bridging oxygens. This second possible symmetry of the metal atoms is shown in lattice images produced by electron micrographs of $Bi_2Sr_2CaCu_2O_{8.2}$, in Fig. 6 of Matsui *et al.*[11] or Fig. 3 in Zandbergen *et al.*[17] (also shown in Fig. 3 of Hewat *et al.*[16]), although those pictures do not show the oxygen atoms. We have recently examined the superstructures of a Co analog[13] and of a Mn analog[18] of the superconductor with one Cu layer per BiO bilayer, which also show a distortion, although with a supercell that repeats in four, instead of five, subcell periods along *a*. These Co and Mn analogs do have mirror symmetry of the metal positions, and two oxygen atoms in bridging positions, and thus confirm this other possible arrangement. In the superconductor, where the modulation is incommensurate, it is likely that the actual oxygen distribution is a random sequence of even and odd numbers of bridging oxygen atoms near the top of the corrugation.

ACKNOWLEDGMENTS

We are grateful to D. M. Hwang for electron microscopy results.

[1]M. A. Subramanian, C. C. Torardi, J. C. Calabrese, J. Gopalakrishnan, K. J. Morrisey, T. R. Askew, R. B. Flippen, U. Chowdhury, and A. W. Sleight, Science **239**, 1015 (1988).

[2]S. A. Sunshine, T. Siegrist, L. F. Schneemeyer, D. W. Murphy, R. J. Cava, B. Batlogg, R. B. van Dover, R. M. Fleming, S. H. Glarum, S. Nakahara, R. Farrow, J. J. Krajewski, S. M. Zahurak, J. V. Waszczak, J. H. Marshall, P. Marsh, L. W. Rupp, Jr., and W. F. Peck, Phys. Rev. B **38**, 893 (1988).

[3]J. M. Tarascon, Y. Le Page, P. Barboux, B. G. Bagley, L. H. Greene, W. R. McKinnon, G. W. Hull, M. Giroud, and D. M. Hwang, Phys. Rev. B **37**, 9382 (1988).

[4]P. Bordet, J. J. Capponi, C. Chaillout, J. Chenevas, A. W. Hewat, E. A. Hewat, J. L. Hodeau, M. Marezio, J. L. Tholence, and D. Tranqui, Physica C **156**, 189 (1988).

[5]H. G. von Schnering, L. Walz, M. Schwarz, W. Becker, M. Hartweg, T. Popp, B. Hettich, P. Muller, and G. Kampf, Angew, Chem. Int. Ed. Engl. **27**, 574 (1988).

[6]C. C. Torardi, J. B. Parise, M. A. Subramanian, J. Gopalakrishnan, and A. W. Sleight, Physica C **157**, 115 (1989).

[7]Y. Gao, P. Lee, P. Coppens, M. A. Subramanian, and A. W. Sleight, Science **241**, 954 (1988).

[8]B. G. Bagley, J.-M. Tarascon, L. H. Greene, P. Barboux, P. Morris, G. W. Hull, M. Giroud, D. M. Hwang, Y. Le Page, and W. R. McKinnon, *Abstracts of the Fall Meeting of the Materials Research Society, 1988* (Materials Research Society, Pittsburgh, 1988).

[9]D. H. Flack, Acta Crystallogr. Sect. A **39**, 876 (1983).

[10]L. D. Landay and E. M. Lifshitz, *Theory of Elasticity,* 2nd ed. (Pergamon, New York, 1970), p. 44.

[11]Y. Matsui, H. Maeda, Y. Tanaka, and Y. Horiuchi, Jpn. J. Appl. Phys. **27**, L372 (1988).

[12]I. D. Brown and D. Altermatt, Acta Crystallogr Sect. B **41**, 244 (1985).

[13]P. Hagenmuller, in *Solid State Chemistry 1982,* edited by R. Metselaar, H. J. M. Heijligers, and J. Schoonman (Elsevier, Amsterdam, 1983), p. 49.

[14]J. Ren, D. Jung, M.-H. Whangbo, J.-M. Tarascon, Y. Le Page, W. R. McKinnon, and C. C. Torardi, Physica C **159**, 151 (1989).

[15]J.-M. Tarascon, P. F. Miceli, P. Barboux, D. M. Hwang, G. W. Hull, M. Giroud, L. H. Greene, Yvon Le Page, W. R. McKinnon, E. Tselepis, G. Pleizier, M. Eibschutz, D. A. Neumann, and J. J. Rhyne, Phys. Rev. B **39**, 11 587 (1989).

[16]E. A. Hewat, J. J. Capponi, and M. Marezio, Physica C **157**, 502 (1989).

[17]H. W. Zandbergen, W. A. Groen, F. C. Mulhoff, C. van Tendeloo, and S. Amelinckx, Physica C **156**, 325 (1988).

[18]E. Tselepis *et al.* (unpublished).